

## Article

# Influence of Rainfall Seasonality in Groundwater Chemistry at Western Region of São Paulo State—Brazil

Lais A. Maroubo , Marcos R. Moreira-Silva, José Jerônimo Teixeira and Marcos F. S. Teixeira \* 

Department of Chemistry and Biochemistry, School of Science and Technology—Sao Paulo State University (UNESP), Rua Roberto Simonsen 305, Presidente Prudente, SP 19060-900, Brazil; lmaroubo@hotmail.com (L.A.M.); silvajr.mrm@gmail.com (M.R.M.-S.); jjteixeirabr@gmail.com (J.J.T.)

\* Correspondence: marcos.fs.teixeira@unesp.br

**Abstract:** The present study evaluated the spatiotemporal variation in concentration of cadmium, lead and copper ions in groundwater wells in the stratigraphic subdivision “Santo Anastácio” that belongs to the Bauru aquifer system in the western region of São Paulo State. Exploratory statistics methods were employed to investigate the response of the concentration of these metals in the aquifer through the pluviometric index of the region. The results show a direct dependence of the mean monthly flow of the metals in the groundwaters to the monthly rainfall flow. The observed behavior was cyclic with a gradual increase and decrease in the flow throughout time. Two groups of cyclic variation were identified. The seasonality of the mean monthly flow of  $\text{Cd}^{2+}$  and  $\text{Pb}^{2+}$  was inversely proportional to the magnitude of the pluviometric index of the region studied. Meanwhile, the seasonality of  $\text{Cu}^{2+}$  was directly correlated to the seasonable rainfall variability. These behaviors lead us to point out that cadmium and lead come from minerals present in the aquifer itself and the presence of copper in groundwater is associated with an anthropogenic action due to the region’s agricultural activity. The study helps us better comprehend the behavior of the whole groundwater system through a comparison with temporal hydrogeochemistry.

**Keywords:** spatiotemporal distribution; metal transport; correlation analysis; groundwater



**Citation:** Maroubo, L.A.; Moreira-Silva, M.R.; Teixeira, J.J.; Teixeira, M.F.S. Influence of Rainfall Seasonality in Groundwater Chemistry at Western Region of São Paulo State—Brazil. *Water* **2021**, *13*, 1450. <https://doi.org/10.3390/w13111450>

Academic Editor: Aldo Fiori

Received: 18 February 2021

Accepted: 19 May 2021

Published: 21 May 2021

**Publisher’s Note:** MDPI stays neutral with regard to jurisdictional claims in published maps and institutional affiliations.



**Copyright:** © 2021 by the authors. Licensee MDPI, Basel, Switzerland. This article is an open access article distributed under the terms and conditions of the Creative Commons Attribution (CC BY) license (<https://creativecommons.org/licenses/by/4.0/>).

## 1. Introduction

The exploitation of groundwaters has been taking great proportions due to its various advantages, such as the quality of the water, the costs of the exploitation and the reduction in the treatment phases until it reaches the final consumer. Its use for public supply has gained significant relevance in areas where surface water is scarce. The increase in its consumption is mainly due to populational growth, climate changes, which cause a shortage of surface water, and the increase of surface water pollution [1–4].

Groundwater reserves are a dynamic resource subjected to qualitative and quantitative modifications as a result of various contamination sources (e.g., agricultural, industrial and domestic) [5–7]. The quality and characteristics of groundwaters are a function of natural processes (e.g., geology, groundwater flow direction, quality of groundwater recharge/water and rock interactions), anthropogenic activities (e.g., agricultural production, industrial growth, urbanization with an increase in groundwater exploitation) and atmospheric input [4,8–10]. The index of potentially toxic elements discard has been intensified especially due to irregular discard in natural reservoirs through anthropogenic actions, such as mining, industrialization, irregular landfill constructions, indiscriminate usage of pesticides and fertilizers in agriculture, domestic sewage, etc. The presence of these potentially toxic elements is responsible for adverse effects in the environment, causing damage to public health and the economy [11]. Apart from anthropogenic actions, the insertion of potentially toxic metals in aquatic systems occurs naturally through geochemical processes like weathering, the region’s geological structure and climate changes, in addition to the interaction of atmospheric particulate matter in the rain composition and its interactions

when there is the percolation of this water in the soil, mixing into the existing aquifers throughout the leaching course in soil [12,13].

Facing the enormous importance of groundwater previously mentioned, countless researches towards identification and quantification of potentially toxic metals in hydrographic basins and aquifers have been conducted [14,15]. The seasonality of rainfall affects dynamically the conditions of groundwater quality and quantity, resulting in alterations in the redox conditions, in the concentrations of substances *in situ* and the levels of water in the aquifer. Studies of seasonal identification and spatial variation of the anthropogenic and natural effects aiming to improve and comprehend hydrogeochemical processes based on pluviometric indexes have been described in the literature [16–20]. In this present paper, we present the identification of seasonable characteristics and spatial variations in the natural and anthropogenic effects aiming to improve and comprehend hydrochemical processes of groundwater in the western region of São Paulo State. The study was conducted for 17 months following the variations in concentrations of lead, cadmium and copper in groundwaters.

## 2. Methods

### 2.1. Study Area

The study area is located in the west of the São Paulo State—Brazil. With an area of approximately 17,500 km<sup>2</sup> and an estimated population of about 540,000 inhabitants (demographic density of 30.76 inhabitants/km<sup>2</sup>), where the Presidente Prudente municipality stands out as a major regional economic pole, the economy is based on agriculture, livestock, industry and commerce. The area belongs to the geomorphological province called Planalto Ocidental Paulista and the relief is characterized by a succession of smoothed hills composed of sandstone spikes. According to the Köppen classification [21], the climate in the Presidente Prudente region is Aw: mesothermal with hot summers and dry winters, annual rainfall, with an average of 130 mm (driest month in July, with an annual average of 39 mm), average temperature of the warmest month (February) of 25.5 °C and that of the coldest month (June) of 20 °C.

The hydrogeological study area is based on the Bauru Aquifer System highlighted as a green area on the map of the São Paulo State (Figure 1), composed of the Marília, Adamantina, Araçatuba, Santo Anastácio and Caiuá aquifers [22]. The system behaves as a hydrogeological unit of regional extension, continuous, free and locally confined. Groundwater was collected from the Santo Anastácio aquifer. The Santo Anastácio Aquifer emerges in a narrow strip parallel to the Paraná River (yellow highlighted in Figure 1), but on a subsurface it advances in an easterly direction, extending for approximately 67,000 km<sup>2</sup>.

The Santo Anastácio Formation consists predominantly of very fine to medium-grained sandstones, rounded to sub-angular grains, reddish-brown in color, ferruginous and locally carbonate cementation. It is poor in sedimentary structures, with massive strata with a maximum thickness of 80 m, with incipient plane-parallel stratification. Regarding the classification from the point of view of chemical composition, the aquifer has a predominance of calcium or magnesium bicarbonated water. The aquifer transmissivity is around 50 to 100 m<sup>2</sup>/day.

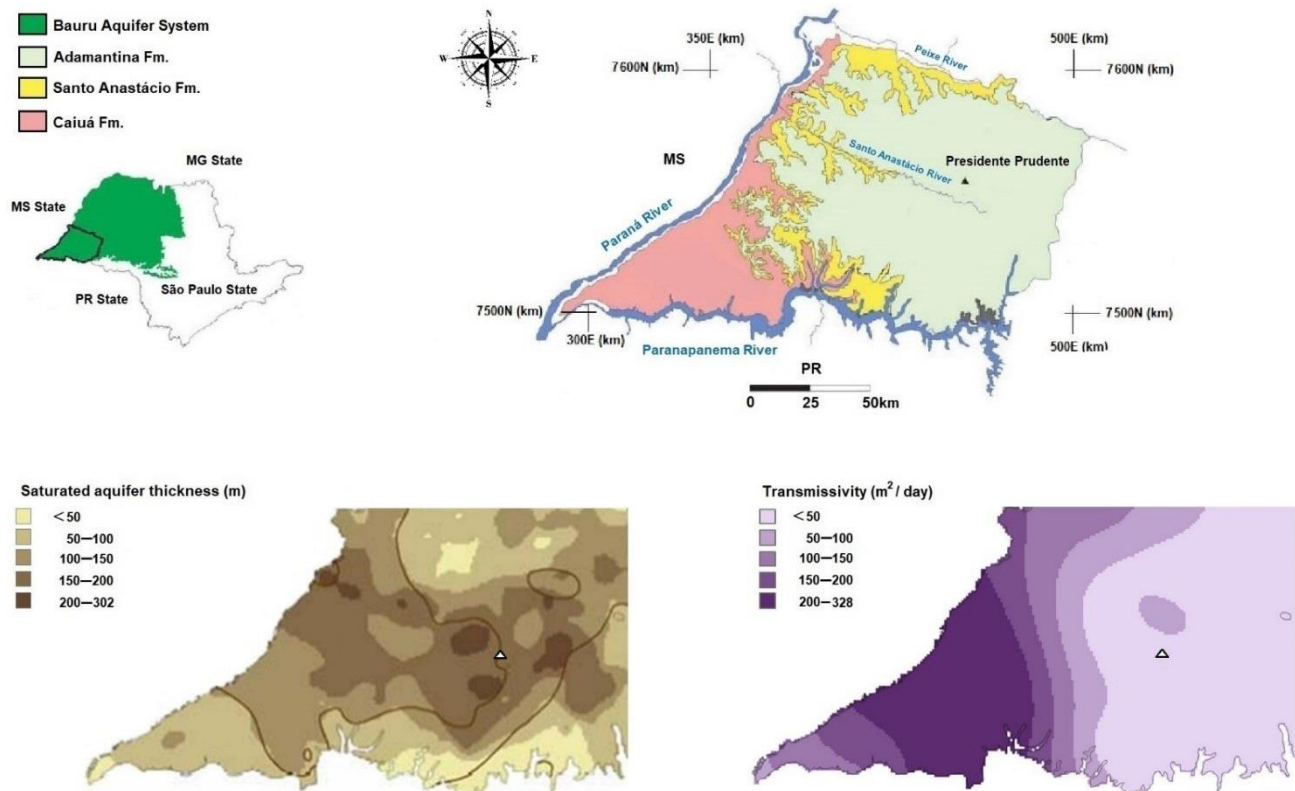


**Figure 1.** Hydrogeologic map of the Bauru Group in São Paulo state showing its outcropping lithostratigraphic units which correspond to homologous hydrogeologic units in the study area (modified from Ref. [22]). Highlighting the saturation and transmissivity of the Bauru Aquifer System in the portion of the study area.

### 2.2. Groundwater Sampling and Analysis

Groundwater samples were collected from 7 monitoring wells over a period of 17 months from August 2017 to December 2018. The sampling points were identified by W1, W2, W3, W4, W5, W6 and W7 (Figure 2). Samples were collected every two weeks throughout the collection months. Table 1 presents the data and characteristics of the locations where the collections were performed (points 1 to 7).

Samples were collected after pumping based on the International Standard MSZ EN ISO 5667–1. In the field, temperature and pH were measured in a Metrohm pH meter. The concentrations of copper, lead and cadmium in water were determined by differential pulse stripping voltammetry, according to the Metrohm procedure (VA Application Note n° V-86 version 01). All measurements were made in triplicate, the reproducibility of the analytical data was 5%. Results were statistically characterized and analyzed using Excel 2016 and Origin 2019 statistical software (OriginLab Corporation, Northampton, MA, USA).

**Table 1.** Characteristics of the areas where were acquired as sampling.

Point	W1	W2	W3	W4	W5	W6	W7
	22°08′32.98″ S 51°27′49.79″ W	22°9′0.14″ S 51°25′23.60″ W	22°05′47.72″ S 51°25′42.95″ W	22°07′11.62″ S 51°24′50.49″ W	22°07′20.57″ S 51°24′30.98″ W	22°07′21.18″ S 51°24′29.77″ W	22°07′31.86″ S 51°24′42.25″ W
Altitude (m)	435	420	449	408	446	445	422
Depth (m)	120	110	175	195	170	190	172
Use	Irrigation	Human consumption Residential area.	Human consumption	Recreation	Maintenance and sanitation	Irrigation	Public supply
Local aspect	Green area. Low population flow.	High vehicular and population flow.	Green area.	Residential area. High vehicular and population flow.	Green area. High vehicular and population flow.	Green area. High vehicular and population flow.	Urbanized area.

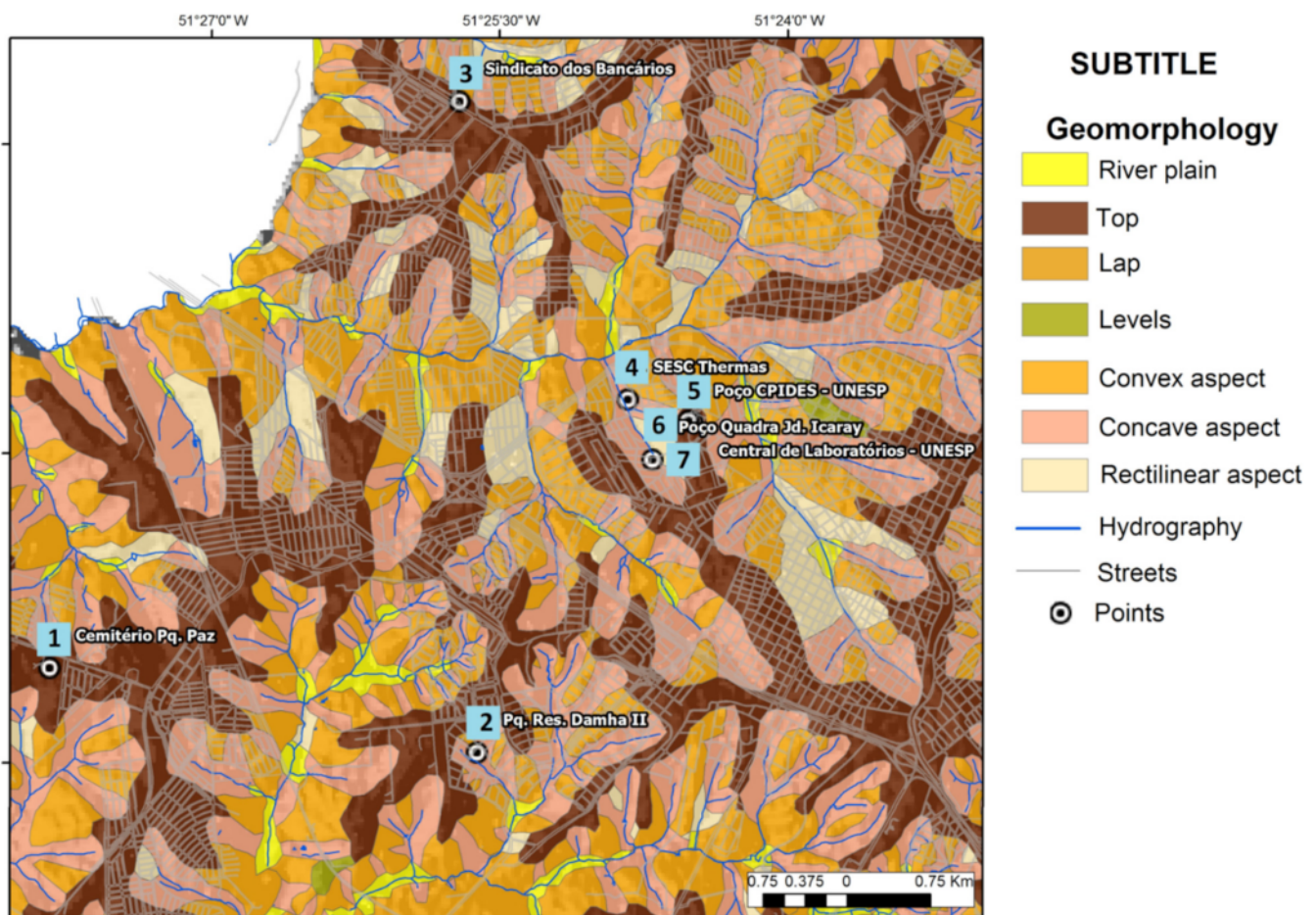


Figure 2. Location of sampling wells in the study area.

### 3. Results and Discussion

The employment of exploratory statistics aimed to estimate the degree of variability assuming that the variables studied are affected by the pluviometric index. Thus, the discussion in the present paper is distributed in topics to each biweekly analyzed chemical component in groundwater.

#### 3.1. Spatiotemporal Distribution and Exploratory Statistic of Cadmium in Groundwater

From the data obtained in the analysis of  $\text{Cd}^{2+}$  concentration, a basic descriptive statistic was performed (minimum, maximum, mean, standard deviation and median values) to understand the relation between the main parameters and the sampled wells in the research field. The values of mean monthly cadmium flow, among all wells, varied from 1.48 to  $44 \mu\text{g L}^{-1}$ . Table 2 presents the mean monthly values and their respective standard deviations of the obtained concentrations in the samples, as well as the values of minimum, maximum, mean, standard deviation and median in each well during the period studied.

The influence of the spatiotemporal behavior of the aquifer hydraulic charge on the mean monthly cadmium concentration was correlated to the parameter of mean monthly pluviometric level of the study region as if it was the recharge level or water volume level of the aquifer [23]. A Figure 3A shows a seasonable or cyclic behavior of the increasing and decreasing in the mean monthly flow of the mentioned metallic cation throughout time. With a statistical technique to aid the data interpretation, a trend curve was elaborated

(short-dash-dot curve of Figure 3A) for the cadmium concentration in the aquifer in a temporal function in which the analysis occurred.

**Table 2.** Mean monthly cadmium concentration ( $\mu\text{g L}^{-1}$ ) with standard deviation value determined for each studied well (W) during the 17 months.

Month	W1	W2	W3	W4	W5	W6	W7
Aug/XX	12.7 ± 2.7	5.40 ± 3.29	38.5 ± 1.2	24.1 ± 5.6	10.2 ± 0.3	15.3 ± 4.4	19.9 ± 5.2
Sep/XX	9.93 ± 3.84	18.8 ± 1.2	44.0 ± 6.4	26.6 ± 0.8	33.9 ± 5.6	30.1 ± 8.3	23.8 ± 1.1
Oct/XX	6.63 ± 0.83	10.2 ± 2.9	15.6 ± 4.0	23.5 ± 3.7	17.6 ± 3.7	11.8 ± 4.6	7.58 ± 2.99
Nov/XX	4.48 ± 0.77	7.55 ± 0.39	3.24 ± 0.72	8.20 ± 0.37	5.76 ± 1.65	6.34 ± 0.75	3.48 ± 0.09
Dec/XX	2.03 ± 1.40	2.22 ± 1.46	2.39 ± 0.14	7.09 ± 0.51	2.63 ± 1.74	5.33 ± 0.35	1.48 ± 0.16
Jan/YY	1.75 ± 0.29	1.57 ± 0.51	1.87 ± 0.29	2.53 ± 0.73	3.74 ± 0.14	1.52 ± 0.15	1.99 ± 0.31
Feb/YY	3.78 ± 0.17	2.80 ± 0.09	2.54 ± 0.45	3.41 ± 0.48	3.94 ± 0.11	2.18 ± 0.24	3.02 ± 0.07
Mar/YY	4.71 ± 0.27	4.25 ± 0.67	3.22 ± 0.09	3.94 ± 0.06	5.46 ± 0.37	3.55 ± 0.04	5.08 ± 0.22
Apr/YY	6.05 ± 0.53	5.65 ± 0.10	4.15 ± 0.67	5.06 ± 0.95	6.99 ± 0.02	3.97 ± 0.26	6.05 ± 0.40
May/YY	8.80 ± 0.57	8.16 ± 0.35	6.03 ± 0.93	7.44 ± 1.19	8.55 ± 1.13	7.10 ± 0.30	8.10 ± 1.19
Jun/YY	11.4 ± 0.1	9.81 ± 0.60	8.27 ± 0.34	12.2 ± 4.4	11.8 ± 1.0	10.1 ± 0.1	10.9 ± 1.8
Jul/YY	13.9 ± 0.2	12.7 ± 2.7	25.9 ± 3.8	18.9 ± 0.2	14.1 ± 0.3	13.6 ± 3.4	20.2 ± 2.4
Aug/YY	17.2 ± 7.0	13.11 ± 9.1	33.3 ± 6.5	22.5 ± 3.7	16.3 ± 7.4	19.6 ± 6.4	24.1 ± 6.6
Sep/YY	15.7 ± 5.9	15.7 ± 3.6	40.3 ± 5.6	22.7 ± 4.6	28.9 ± 7.5	32.0 ± 6.2	26.9 ± 6.0
Oct/YY	7.10 ± 1.87	8.45 ± 2.74	19.5 ± 5.6	20.2 ± 4.6	14.05 ± 4.9	14.6 ± 4.7	9.71 ± 4.0
Nov/YY	3.98 ± 0.73	6.01 ± 1.84	5.72 ± 2.93	7.87 ± 0.49	4.50 ± 1.79	6.05 ± 1.10	4.91 ± 1.71
Dec/YY	1.76 ± 0.87	2.12 ± 1.17	4.74 ± 2.73	4.65 ± 2.95	2.51 ± 1.01	3.99 ± 1.84	3.40 ± 2.23
Average *	7.76 ± 4.96	7.91 ± 4.99	15.2 ± 15.1	13.0 ± 8.7	11.2 ± 9.0	11.0 ± 9.1	10.6 ± 8.7
Minimum	1.75	1.57	1.87	2.53	2.51	1.52	1.48
Median	6.63	7.55	6.03	8.20	8.55	7.10	7.58
Maximum	17.2	18.8	44.0	26.6	33.9	32.0	26.9

\* Average value per well.

Through the model, we can observe that the cadmium concentration exhibits a crescent tendency in the dry season (April through September) and a decrescent tendency in the rainy season (October through March). The transformation of the concentration data and pluviometric index to the logarithmic base (see Figure 3B) demonstrates correlative and significative cycles in both parameters analyzed in temporal sampling function. The model indicates that the phenomenon has a periodicity, or it obeys a periodical function, where the mean logarithmic concentration of cadmium is inversely proportional to the magnitude of the monthly seasonable variability of rainfall. The cyclic variation in the cadmium mean monthly flow is indicative that the chemical element does not come from an external source and it is found in the aquifer's area itself. During the rainy season, there is a dilution effect due to the increase in the aquifer's water volume. Meanwhile, during the dry season, the low water level in the aquifer causes the opposite process, when the cadmium concentration increases.

Figure 4 presents a boxplot diagram [24] that provides a better representation of the observed data variation in each well for the cadmium concentration during the dry (Figure 4A) and rainy seasons (Figure 4B). The distinction between the rainy and dry seasons is very clear as it is shown in both boxplot diagrams. A general seasonal distinction is based on the only components from the hydric balance on a monthly scale as shown in Figure 3B. Analyzing the dataset of each well during the dry season (Figure 4A), well W3 presents the highest dispersion on the values of cadmium concentration in the interquartile range, which consists in a difference between the third and the first quartile. One of the concentration variability factors is the process of groundwater pumping during the driest seasons, influenced by the extremely low levels of the groundwater, resonating significantly in the chemical compound's concentration in the aquifer [16]. Comparatively, the lowest dispersion in the interquartile range for the values of cadmium concentration was observed in the well W1. A factor for the lowest dispersion in the concentration of cadmium may be related to the location of the well W1 that is situated in a green area with a low population

density. Analyzing the median lines, the wells W5 and W6 present a positive asymmetric distribution, indicating that the median is close to the first quartile or that the median value is lower than the mean value. Meanwhile, the wells W2, W3, W4 and W7 present a negative asymmetric distribution. It was verified for the well W1 that the mean and median values are coincidental demonstrating a symmetric distribution. It is important to point out that the median is the central tendency measure more appropriate when the data present asymmetric distribution since the arithmetic mean is influenced by the extreme values.

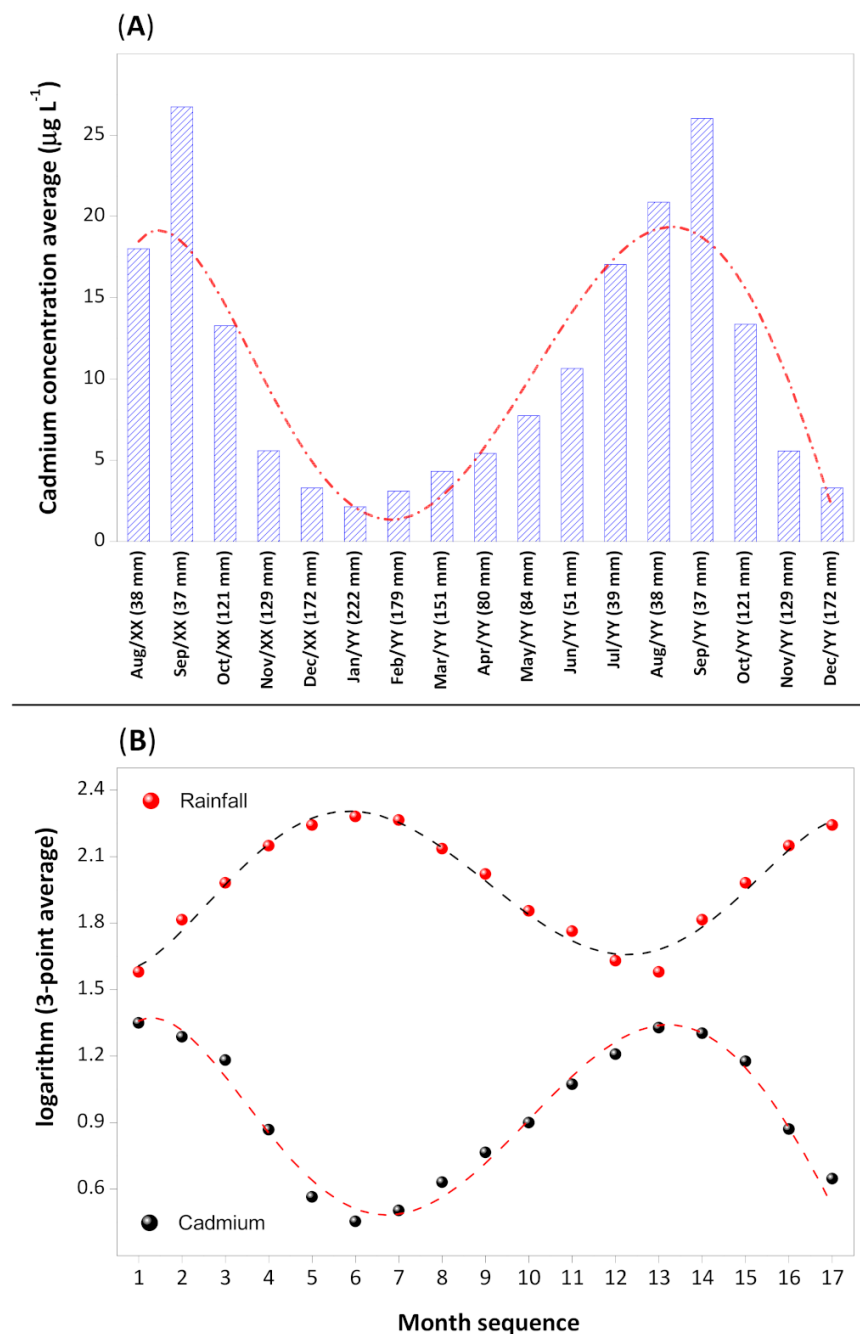


**Figure 3.** (A) Average temporal evolution of average cadmium concentration ( $n = 7$ ) and the pluviometric levels ( $n = 39$ ) in accordance with the seasonal period. The red short-dash-dot curve corresponds to the trend curve of the variability of cadmium concentration in the aquifer during the 17 months of study. (B) Normalized flow of cadmium concentration (black circle) and pluviometric index (red circle) throughout the sampling period. The results are presented as the mean value of 3 point.

Contrastingly, cadmium concentration is lower in groundwater collected during the rainy season (Figure 4B) with a mean monthly below  $10 \mu\text{g L}^{-1}$ . As previously shown in Figure 3B, this result is due to the dilution of the concentration by groundwater recharge. However, the descriptive parameters in the boxplots present anomalous values (outliers) in almost every well studied (except in wells W1 and W2). The anomalous values are related to the first rainy month (October) in which the cadmium concentrations are still high in comparison to the dataset for the period, implying that the dilution factor is in the initial phase in the aquifer due to the dependence of the groundwater recharge rate [25].

Table 3 presents mean values for the monthly rainfall index (MRI), pH and cadmium concentration. The monthly mean values of pH were calculated based on the pH measurements of groundwater in each well studied.

**Table 3.** Monthly rainfall index (MRI), mean monthly cadmium(II) concentration and mean monthly pH values determined by the average of all studied wells.

Month	MRI (mm)	Mean [Cd] ( $\mu\text{g L}^{-1}$ )	Mean pH Value
Aug/XX	38	$18.0 \pm 10.9$	$7.97 \pm 1.15$
Sep/XX	37	$26.7 \pm 10.9$	$8.03 \pm 1.08$
Oct/XX	121	$13.3 \pm 6.0$	$7.93 \pm 1.06$
Nov/XX	129	$5.58 \pm 1.9$	$7.84 \pm 1.31$
Dec/XX	172	$3.31 \pm 2.07$	$7.92 \pm 0.91$
Jan/YY	222	$2.14 \pm 0.78$	$8.54 \pm 1.16$
Feb/YY	179	$3.09 \pm 0.65$	$8.43 \pm 0.78$
Mar/YY	151	$4.32 \pm 0.81$	$8.43 \pm 1.30$
Apr/YY	80	$5.42 \pm 1.09$	$8.26 \pm 1.34$
May/YY	84	$7.74 \pm 0.96$	$8.26 \pm 1.08$
Jun/YY	51	$10.6 \pm 1.36$	$8.17 \pm 1.36$
Jul/YY	39	$17.0 \pm 4.8$	$8.22 \pm 1.08$
Aug/YY	38	$20.8 \pm 6.6$	$8.24 \pm 1.14$
Sep/YY	37	$26.0 \pm 8.9$	$7.99 \pm 1.33$
Oct/YY	121	$13.4 \pm 5.2$	$7.68 \pm 1.08$
Nov/YY	129	$5.58 \pm 1.3$	$7.59 \pm 1.31$
Dec/YY	172	$3.31 \pm 1.2$	$7.67 \pm 0.91$

To verify the dependence degree of the mean monthly flow to the rainfall index and the pH of the water collected, Pearson correlation coefficient was applied with paired Student's *t*-test with a significance level of 5% on the correlation coefficient obtained, where  $H_0: r = 0$  and  $H_1: r \neq 0$ . As shown in Table 4, there is a moderate relation between the MRI parameters and the mean cadmium concentrations in groundwater.

**Table 4.** Pearson correlation coefficient matrix for monthly rainfall index (MRI), cadmium(II) concentration and pH values for 17 months.

	MRI	Mean Cd	Mean pH	Correlation	R <sup>2</sup>	n
MRI	1					12
Mean Cd	-0.70161	1		moderate	0.4923	17
Mean pH	0.03187	-0.09685	1	weak	0.0094	17

Comparing the calculated *t* value ( $-5.352$ ) to the critical value for the Student's *t*-distribution ( $\pm 2.131$ ), *t* value is out of the region for the  $H_0$  hypothesis to be accepted. Thus, we can conclude that there is enough evidence to correlate the concentration parameters of Cd(II) to MRI. Concerning the mean monthly of Cd(II) and the mean pH, the Pearson coefficient obtained shows that there is a weak relation. Comparing the calculated *t* value ( $-0.379$ ) to the critical value for the Student's *t*-distribution ( $\pm 2.131$ ), *t* value is in the region for the  $H_0$  hypothesis to be accepted. Thus, we can conclude that there is not enough evidence suggesting that there is a relation between the cadmium concentration

and the pH. The statistical result obtained through Pearson’s correlation indicates that the variability in groundwater pH is not caused by the variation in cadmium concentration in function of the region’s rainfall index.

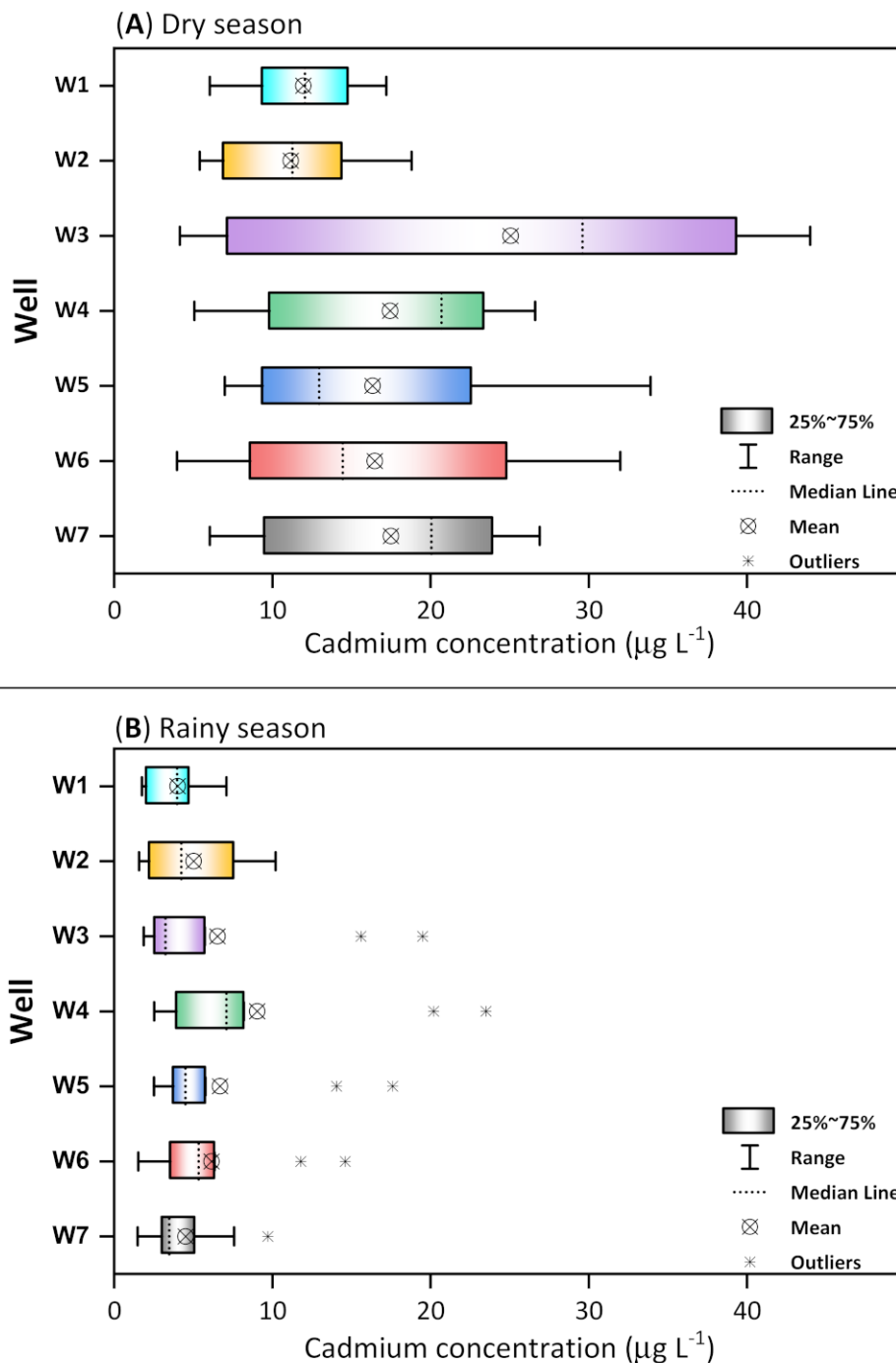


**Figure 4.** Boxplot diagram for cadmium concentration in 7 wells during the 17 months of study. (A) Dry season and (B) Rainy season. Lines and crosses within boxes represent the median and mean, respectively. The asterisk corresponds to outlier (atypical values).

### 3.2. Spatiotemporal Distribution and Exploratory Statistic of Lead in Groundwater

Table 5 presents the mean monthly values and their respective standard deviations of the obtained samples concentrations, as well as minimum, maximum, mean, standard deviation and median values in each well for study period.

**Table 5.** Mean monthly lead(II) concentration ( $\mu\text{g L}^{-1}$ ) with standard deviation value determined for each studied well (W) during the 17 months.

Month	W1	W2	W3	W4	W5	W6	W7
Aug/XX	35.2 ± 9.6	27.2 ± 0.7	19.3 ± 3.4	22.9 ± 2.6	26.7 ± 5.6	24.2 ± 1.8	23.0 ± 3.2
Sep/XX	18.7 ± 11.4	19.9 ± 0.2	37.7 ± 13.1	16.9 ± 3.1	28.2 ± 7.9	40.5 ± 5.5	23.4 ± 2.1
Oct/XX	7.30 ± 0.50	14.3 ± 3.51	8.18 ± 0.71	8.67 ± 0.15	19.0 ± 4.4	13.5 ± 1.6	10.2 ± 1.9
Nov/XX	4.05 ± 0.23	9.49 ± 0.69	6.23 ± 1.86	3.93 ± 0.23	8.12 ± 1.10	5.77 ± 0.47	6.27 ± 0.55
Dec/XX	2.07 ± 0.59	3.50 ± 0.46	2.17 ± 0.20	1.46 ± 0.60	4.32 ± 0.59	3.39 ± 0.59	1.39 ± 0.13
Jan/YY	2.77 ± 0.14	3.56 ± 1.10	2.06 ± 0.36	2.24 ± 0.25	3.54 ± 0.60	1.73 ± 0.75	3.39 ± 1.02
Feb/YY	6.67 ± 1.72	5.00 ± 0.55	2.86 ± 0.17	3.49 ± 0.31	4.79 ± 0.48	2.89 ± 0.21	4.85 ± 0.47
Mar/YY	8.50 ± 0.74	8.09 ± 0.40	3.49 ± 0.18	3.91 ± 0.10	6.08 ± 0.15	3.82 ± 0.06	5.36 ± 0.16
Apr/YY	12.5 ± 4.8	10.3 ± 0.3	4.80 ± 0.13	4.82 ± 0.81	6.95 ± 0.11	4.23 ± 0.08	5.85 ± 0.13
May/YY	16.8 ± 0.4	11.5 ± 0.7	7.41 ± 1.78	8.73 ± 2.33	10.7 ± 2.8	6.52 ± 0.84	6.72 ± 0.53
Jun/YY	17.4 ± 0.1	20.0 ± 3.4	11.0 ± 0.6	14.4 ± 0.24	16.3 ± 0.8	9.05 ± 1.14	9.56 ± 2.70
Jul/YY	23.0 ± 3.2	37.4 ± 5.35	13.4 ± 2.1	16.4 ± 0.29	44.9 ± 4.4	16.3 ± 6.5	17.8 ± 1.89
Aug/YY	33.7 ± 6.9	41.6 ± 8.5	18.6 ± 2.9	22.5 ± 1.65	41.1 ± 0.9	37.8 ± 4.9	25.4 ± 5.3
Sep/YY	23.4 ± 2.1	16.7 ± 4.4	35.5 ± 8.8	18.3 ± 2.5	32.7 ± 6.1	34.3 ± 9.0	29.4 ± 7.2
Oct/YY	12.2 ± 1.1	10.8 ± 4.5	8.94 ± 1.10	11.5 ± 3.8	13.5 ± 6.7	16.2 ± 6.4	12.2 ± 5.1
Nov/YY	8.80 ± 2.75	6.77 ± 3.17	7.44 ± 1.77	7.09 ± 3.66	7.17 ± 1.66	6.92 ± 1.53	6.50 ± 2.12
Dec/YY	2.62 ± 1.61	2.78 ± 0.60	3.04 ± 1.02	4.46 ± 3.71	3.24 ± 0.20	4.54 ± 2.21	3.36 ± 2.28
Average *	13.9 ± 10.3	14.6 ± 11.5	10.1 ± 7.1	11.3 ± 10.8	16.3 ± 13.6	13.6 ± 12.9	11.24 ± 8.8
Minimum	2.07	2.78	1.46	2.06	3.24	1.73	1.39
Median	12.2	10.8	8.7	7.44	10.7	6.92	6.72
Maximum	35.2	41.6	22.9	37.7	44.9	40.5	29.4

\* Average value per well.

The mean monthly lead flow variation (minimum =  $1.39 \mu\text{g L}^{-1}$  and maximum =  $44.9 \mu\text{g L}^{-1}$ ) in the wells was similar to what was observed for the cadmium concentrations. The concentration magnitude varied with the monthly period of the sampling and the geographical position of the wells studied. With the obtained data of lead concentrations, a spatiotemporal graph for the variation in total mean lead concentration was plotted in the logarithmic base (Figure 5B).

The profile of lead concentration variation in groundwater followed a periodicity model in function of time and the highest concentration magnitudes were observed during the dry season. Analyzing comparatively the lead spatiotemporal behavior, we can conclude that this element is found in the aquifer itself. Its dilution in the groundwater is due to increasing in hydric volume and consequently to the recharge flow (pluviometric level). For better visualization of what was verified before, Table 6 presents the lead mean concentration in wells W1 to W7 with their respective standard deviations, in the rainy season (October through March) and in the dry season (April through September). Evaluating the boxplot diagram, the highest dispersions and lead concentration distributions were observed during the dry season (Figure 6A). As observed before, well W1 presented the lowest variability of concentration in the sampling temporal scale. In general, the medians are very close to the concentration means, indicating that the observed concentrations in the dry season are a symmetrical normal distribution. For the rainy season, the mean monthly lead flow values (Figure 6B) were below  $10 \mu\text{g L}^{-1}$ . However, outlier concentrations were observed in wells W5, W6 and W7 and these outlier values correspond precisely to the beginning of the rainy season.

In the Pearson test to analyze the dependence degree of  $\text{Pb}^{2+}$  concentration to the mean pH of the collected water, with a correlation coefficient ( $\rho$ ) of  $-0.0066$ , there is an indication that these two variables are not correlated. To confirm that the variability in lead concentration is not influenced by the pH or vice versa, a two-tailed Student's *t*-test with a significance level of 5% was applied and considering the null and true hypothesis as  $r = 0$  and  $r \neq 0$ , respectively. Comparing the calculated *t* value ( $-0.26$ ) to the critical value for the Student's *t*-distribution ( $\pm 2.131$ ), the calculated *t* value is in the region for the

H<sub>0</sub> hypothesis to be accepted. Thus, we can conclude that there is not enough evidence to support that Pb<sup>2+</sup> concentration and pH are correlated.

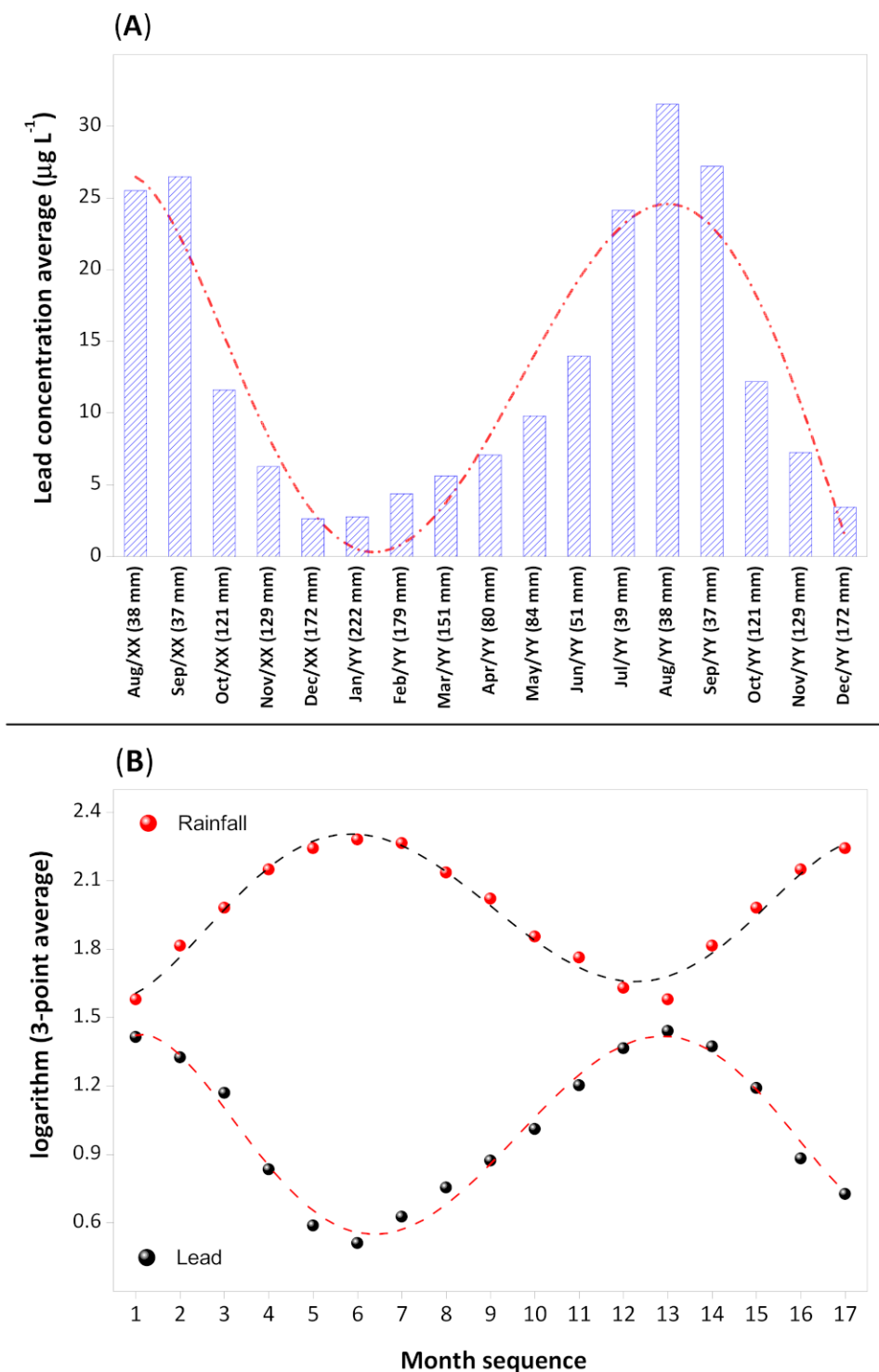


**Figure 5.** (A) Average temporal evolution of average lead concentration (n = 7) and the pluviometric levels (n = 39) in accordance with the seasonal period. The red short-dash-dot curve corresponds to the trend curve of the variability of cadmium concentration in the aquifer during the 17 months of study. (B) Normalized flow of lead concentration (black circle) and pluviometric index (red circle) throughout the sampling period.

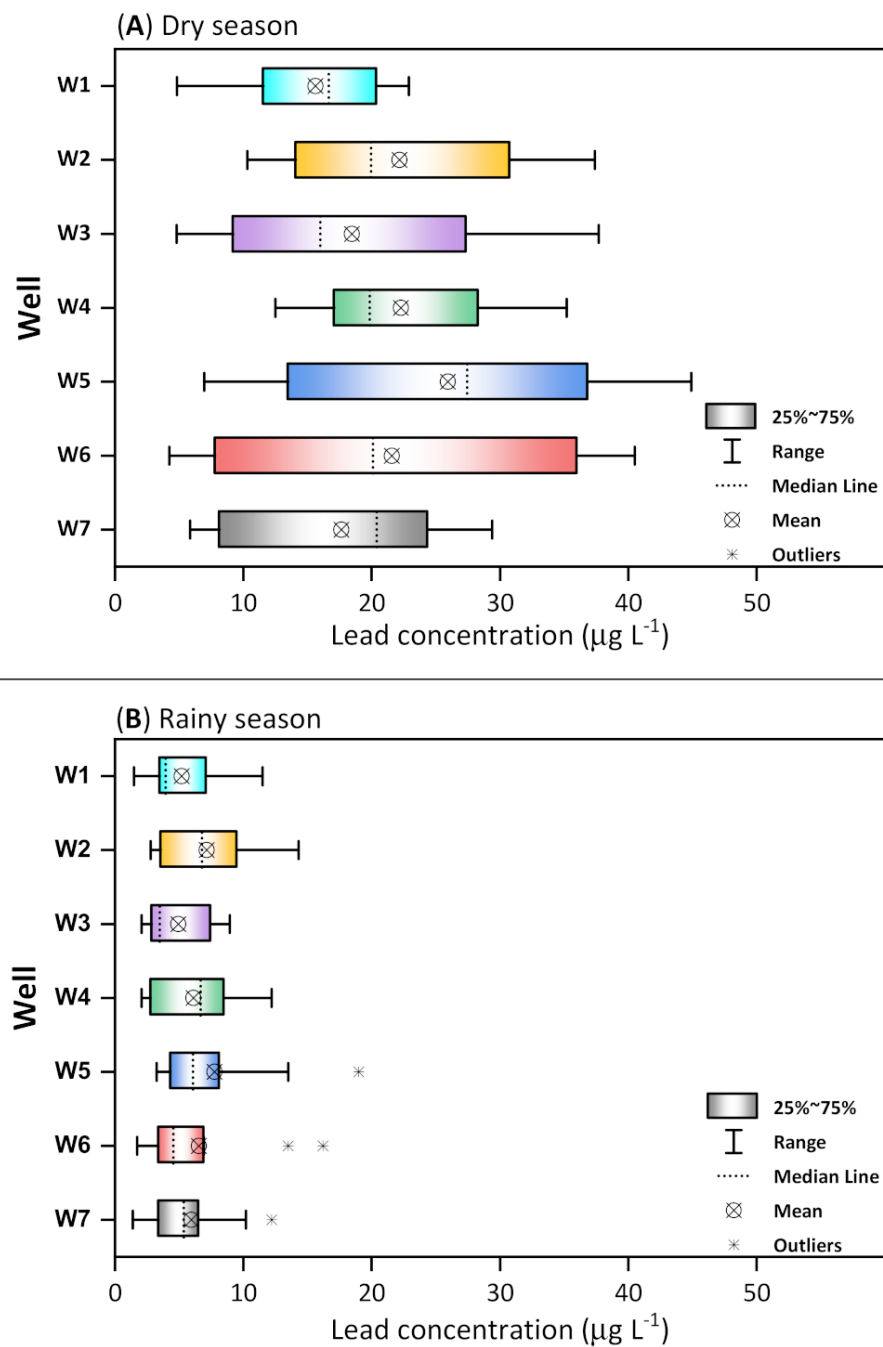


**Figure 6.** Boxplot diagram for lead concentration in 7 wells during the 17 months of study. (A) Dry season and (B) Rainy season. Lines and crosses within boxes represent the median and mean, respectively. The asterisk corresponds to outlier (atypical values).

**Table 6.** Mean total lead(II) concentration by well in dry and rainy season.

Well	Dry	Rainy
W1	22.6 ± 8.1	6.10 ± 3.45
W2	23.1 ± 11.5	7.14 ± 3.89
W3	15.6 ± 6.3	5.19 ± 3.26
W4	18.5 ± 12.2	4.93 ± 2.74
W5	25.9 ± 13.8	7.75 ± 5.26
W6	20.8 ± 14.0	7.10 ± 5.68
W7	18.7 ± 10.7	6.41 ± 3.78

### 3.3. Spatio-Temporal Distribution and Exploratory Statistic of Copper in Groundwater

In the copper concentration spatiotemporal distribution study, it was identified an inverted behavior when compared to the cadmium and lead in groundwater. The mean monthly copper flow values, among all wells, varied from 4.8 to 2.479  $\mu\text{g L}^{-1}$  (see Table 7). In addition, the standard deviation values are higher than the mean, indicating that the copper concentrations are distributed around a wide range of values throughout the entire period.

**Table 7.** Mean monthly copper(II) concentration ( $\mu\text{g L}^{-1}$ ) with standard deviation value determined for each studied well (W) during the 17 months.

Month	W1	W2	W3	W4	W5	W6	W7
Aug/XX	14.5 ± 1.2	24.6 ± 15.5	8.62 ± 2.04	9.03 ± 3.05	9.94 ± 3.32	6.72 ± 0.52	35.2 ± 15.4
Sep/XX	27.5 ± 4.2	32.7 ± 20.0	8.28 ± 7.06	43.6 ± 2.04	4.80 ± 3.59	18.0 ± 1.0	52.3 ± 42.3
Oct/XX	63.5 ± 5.9	86.4 ± 46.1	46.7 ± 3.3	48.1 ± 3.2	23.3 ± 8.5	63.8 ± 43.2	87.9 ± 27.6
Nov/XX	116.3 ± 27.0	181.6 ± 21.5	94.9 ± 9.5	115.1 ± 26.8	93.9 ± 46.6	157.6 ± 1.6	240.4 ± 20.3
Dec/XX	356.9 ± 50.9	333.0 ± 106.1	516.4 ± 168.6	637.0 ± 62.2	344.0 ± 136.2	249.9 ± 122.2	569.6 ± 90.8
Jan/YY	1031 ± 76	2479 ± 167	1060 ± 73	942.5 ± 79.7	925.9 ± 131.4	1949 ± 76	1971 ± 14
Feb/YY	534.2 ± 37.0	867.6 ± 191.8	601.1 ± 39.8	506.6 ± 63.2	553.8 ± 26.3	1207 ± 41	1791 ± 153
Mar/YY	327.1 ± 150.0	365.0 ± 43.8	350.1 ± 36.6	396.4 ± 16.8	404.6 ± 0.4	474.3 ± 5.12	521.0 ± 17.1
Apr/YY	152.0 ± 24.1	265.1 ± 58.0	247.5 ± 56.5	338.9 ± 14.4	337.7 ± 39.2	336.5 ± 65.3	433.7 ± 33.3
May/YY	71.8 ± 17.0	199.1 ± 14.8	129.9 ± 62.7	186.4 ± 62.2	184.0 ± 76.1	144.1 ± 9.4	282.0 ± 98.2
Jun/YY	34.3 ± 13.8	106.6 ± 14.2	41.3 ± 3.0	96.6 ± 0.6	79.5 ± 16.8	27.6 ± 17.6	84.8 ± 2.98
Jul/YY	20.4 ± 3.0	66.2 ± 27.8	27.0 ± 1.8	49.9 ± 9.4	22.4 ± 0.5	9.44 ± 1.53	57.1 ± 7.3
Aug/YY	14.5 ± 1.1	24.6 ± 12.6	8.62 ± 1.7	9.03 ± 2.5	10.0 ± 2.8	6.72 ± 0.42	35.2 ± 12.6
Sep/YY	52.3 ± 4.2	30.1 ± 12.2	25.9 ± 20.8	46.9 ± 4.9	6.53 ± 5.0	11.4 ± 7.9	11.8 ± 7.7
Oct/YY	87.9 ± 2.8	74.9 ± 29.9	47.4 ± 19.4	95.4 ± 57.9	35.0 ± 13.6	43.6 ± 34.2	63.8 ± 43.2
Nov/YY	240.4 ± 20.3	148.0 ± 42.6	105.0 ± 20.1	171.2 ± 71.2	94.4 ± 27.5	125.7 ± 45.6	157.6 ± 1.6
Dec/YY	569.6 ± 90.8	295.0 ± 80.9	426.7 ± 146.6	610.1 ± 150.6	405.2 ± 119.8	222.0 ± 86.3	399.9 ± 89.9
Average *	218.5 ± 275.3	328.2 ± 591.1	220.3 ± 289.1	253.1 ± 275.1	207.9 ± 256.1	297.2 ± 516.7	399.7 ± 586.9
Minimum	14.5	24.6	8.28	9.03	4.8	6.72	11.8
Median	87.9	148	94.9	115.1	93.9	125.7	157.6
Maximum	1031	2479	1060	942.5	925.9	1949	1971

\* Average value per well.

The copper mean monthly concentration through time and its relation of its logarithmic base to the pluviometric index are represented in Figure 7A,B, respectively. Analyzing Figure 7A, it can be observed that the copper concentration in the aquifer increases significantly during the month with higher rainfall intensity. After its concentration peak, the reduction of copper presence in groundwater is gradual and concomitantly with the pluviometric index. Its residence time or memory effect in the aquifer is around 5 months approximately. Through Figure 7B it is possible to observe that the copper concentration in groundwater is directly proportional to the pluviometric level. This behavior indicates strongly that the greater source of copper in groundwater is originated out of the aquifer. It is known that the recharge time can be around days to years depending directly on the hydrogeology properties of the aquifer and of the levels of direct recharge areas. Through the copper variability characterization in groundwater (see Figure 7B), the present study points out that the response of the aquifer's recharge in function of rainfall regime is between 1–2 months, given that the magnitude of the maximum copper concentration is reached after the first period of rainfall. This result corroborates studies of the water table monitoring facing correlations to the pluviometric level in the region [26].

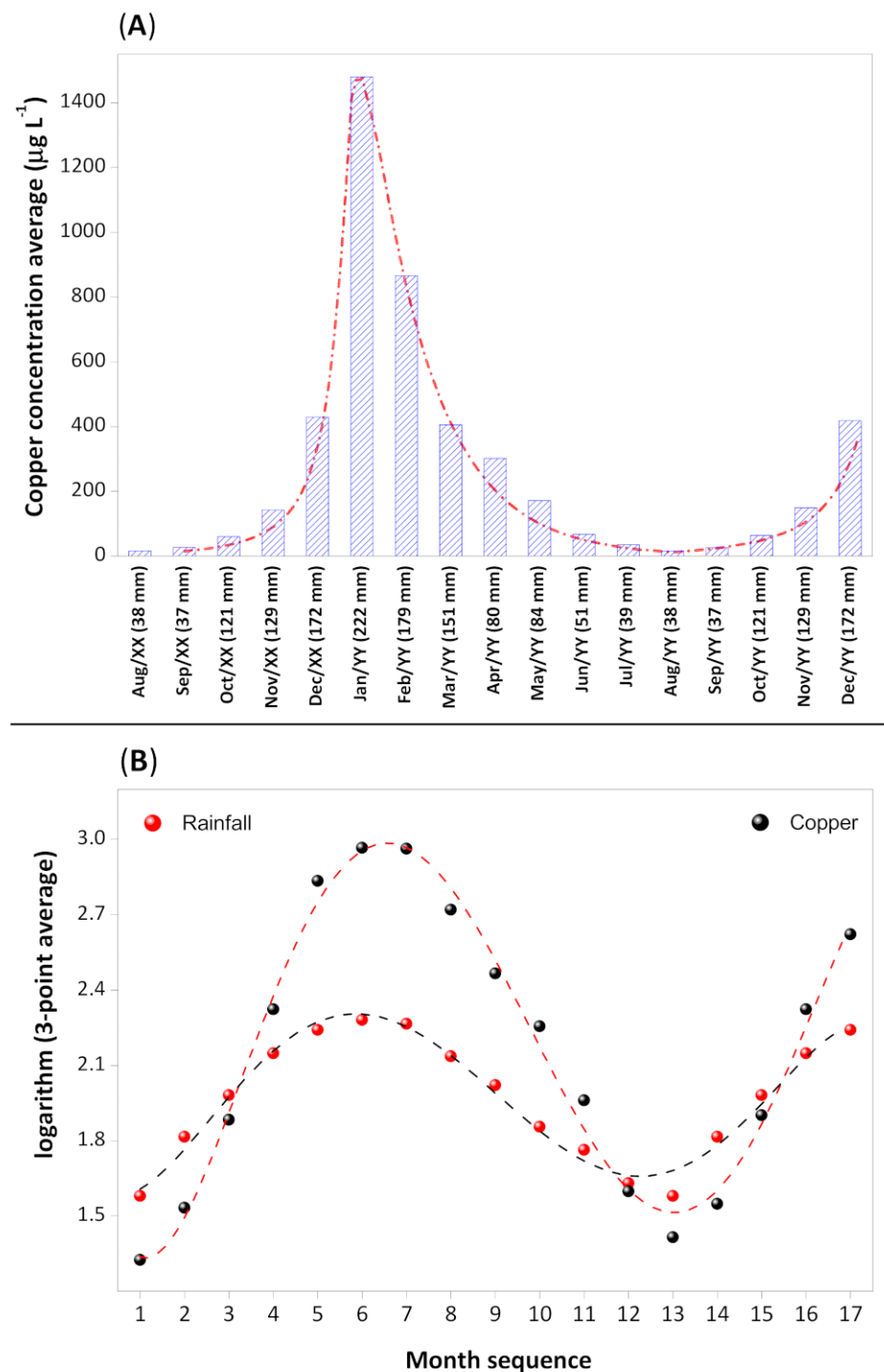


**Figure 7.** (A) Average temporal evolution of average copper concentration (n = 7) and the pluviometric levels (n = 39) in accordance with the seasonal period. The red short-dash-dot curve corresponds to the trend curve of the variability of cadmium concentration in the aquifer during the 17 months of study. (B) Normalized flow of copper concentration (black circle) and pluviometric index (red circle) throughout the sampling period. The results are presented as the mean value of 3 point.

Applying the boxplot diagram (Figure 8) to the copper concentration variability for both pluviometric periods, it is observed more clearly the pluviometric influence when the higher copper concentrations happen during the rainy season (October through March) and its reduction during the dry season (April through September). Differently from the data obtained for cadmium and lead during the dry season, all wells presented

outliers concentrations, which contributed to a higher asymmetric distribution of the data (Figure 8A). This adverse characteristic is related to the beginning of the dry season (April, May and June) when the copper concentration is still relatively high in the aquifer. Through Figure 8B that represents the rainy season, the concentrations magnitudes are about 5 times higher in comparison to the dry season mean. From this observation, it is presented in the item “Conclusion” an analysis of the possible causes of the increase in its concentration during the rainy season. Analyzing the dataset, wells W2, W5, W6 and W7 are the ones that present the higher concentration variability during the rainy season. With the mean monthly pluviometric index values, pH and  $\text{Cu}^{2+}$  concentration, it was verified the dependence degree of these parameters through Pearson’s test. As shown in Table 8, there is a strong correlation between the parameters MRI and copper mean concentrations in groundwater. This conclusion is confirmed through Student’s *t*-test with a significance level of 5%, where  $H_0: r = 0$  and  $H_1: r \neq 0$ . Comparing the calculated *t* value (8.743) to the critical value for the Student’s *t*-distribution ( $\pm 2.131$ ), the calculated *t* value is out of the region for the  $H_0$  hypothesis to be accepted. Thus, we can conclude that there is enough evidence that the parameters of  $\text{Cu}^{2+}$  concentration and mean monthly pluviometric index are correlated.

**Table 8.** Pearson correlation coefficient matrix for monthly rainfall index (MRI), copper(II) concentration and pH values for 17 months.

	MRI	Mean Cu	Mean pH	Correlation	R <sup>2</sup>	n
MRI	1					12
Mean Cu	0.80274	1		strong	0.6444	17
Mean pH	0.03187	0.58840	1	weak	0.3462	17

As for the relation between  $\text{Cu}^{2+}$  concentration and the groundwater pH, the Pearson coefficient value obtained shows that there is a moderated correlation. This conclusion is confirmed by the obtained *t* value (3.486) being higher than the critical value for the Student’s *t*-distribution ( $\pm 2.131$ ), indicating that the calculated *t* value is out of the region for the  $H_0$  hypothesis to be accepted. Thus, we can conclude that the pH of the aquifer is influenced by the presence and concentration of  $\text{Cu}^{2+}$ .

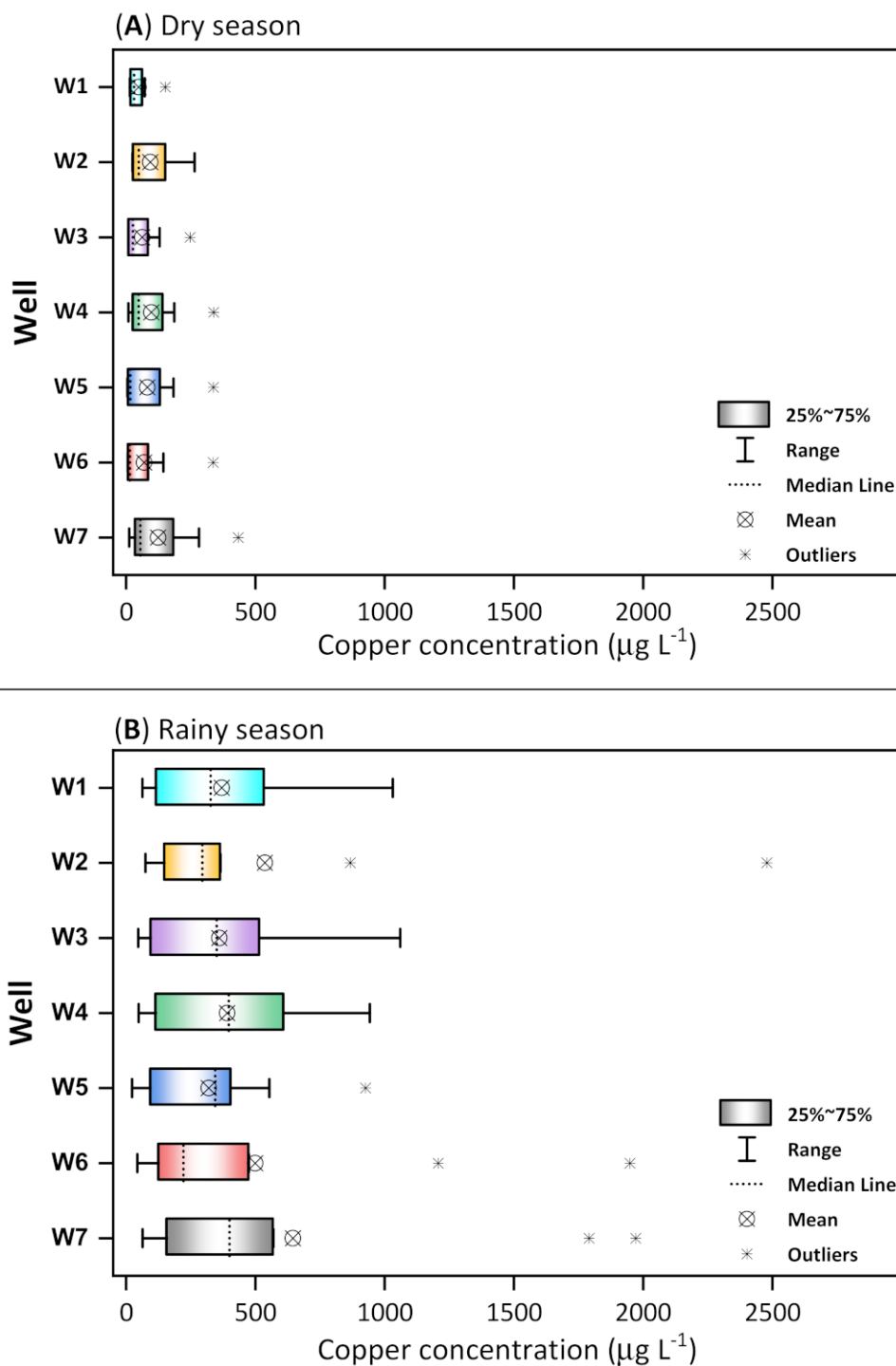


**Figure 8.** Boxplot diagram for copper concentration in 7 wells during the 17 months of study. (A) Dry season and (B) Rainy season. Lines and crosses within boxes represent the median and mean, respectively. The asterisk corresponds to outlier (atypical values).

### 3.4. Principal Component Analysis

A Principal Component Analysis (PCA) was employed to determine the discriminant functions in order to confirm the spatiotemporal variations of chemical elements in groundwater. Table 9 presents two principal components (PC) that obtained the most significant percentage of variability (totalizing 98.3% of the data variability) and the vectors' values per parameter.

**Table 9.** Retention of data variability for the CP1 and CP2 axes and the relationships between cadmium, lead and copper concentrations.

Variable	Cumulative: 98.3%	
	Coefficient of CP1 (82.2%)	Coefficient of CP2 (16.1%)
[Cd <sup>2+</sup> ]	0.60925	0.34847
[Pb <sup>2+</sup> ]	0.60657	0.37380
[Cu <sup>2+</sup> ]	−0.51077	0.85956

The criterion employed in this kind of analysis was the evaluation of the weight of the variable associated with a component. Weights above 0.7 are indicative of strong association; for values between 0.5–0.7, the variable is considered to be moderately associated; weights inferior to 0.5, the variable has a weak association to the component [27]. The first component (82.2%) is associated with a positive moderate variance for cadmium and lead during the dry season. In the same component, the copper variability presented a negative and moderate association for the same period. The second component (16.1%) was strongly associated solely with copper, which can be interpreted as the influence of the rainy season. According to a visual interpretation of the bidimensional representation of the two first principal components (Figure 9), the influence vectors are identified into two groups, as evidenced previously in the exploratory statistics analysis. The variable of copper concentration was close to CP2 axis, showing that the months of January and February (months of the highest pluviometric levels) present high correlations.

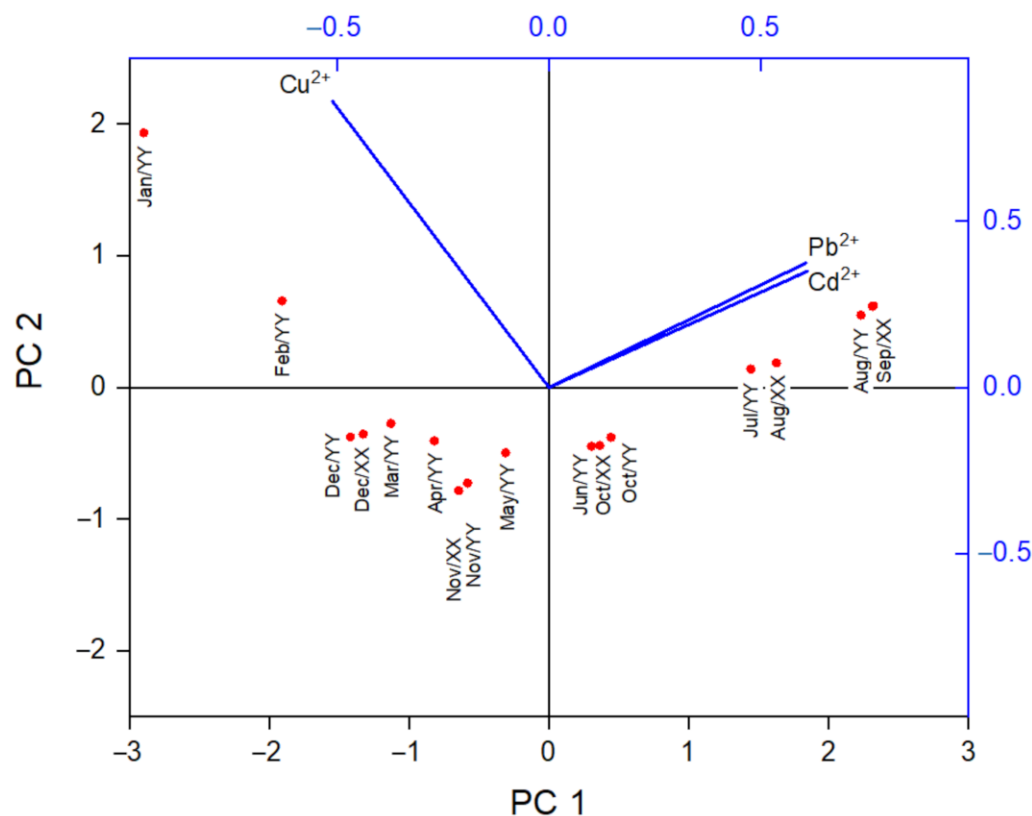


**Figure 9.** Graph of PC1 and PC2 weights for the three observed variables (Cu<sup>2+</sup>; Cd<sup>2+</sup>; Pb<sup>2+</sup>).

Contrastingly, cadmium and lead are more representatives to the CP1 axis, where we can observe that the vectors are equivalent and that the concentrations of these elements are correlative to the months of lowest pluviometric index (July through September). The acute angle of the vectors' points to a high correlation between the two variables.

#### 4. Conclusions

The results obtained through exploratory statistics in cadmium, lead and copper concentration variability provided some information about the processes that control the chemistry of groundwater in the study area. Cadmium and lead ions showed high concentrations in the low pluviometric index period, which can be reintroduced in groundwater through natural interaction water-mineral. During the dry season, the water table becomes lower and more constant [28], causing the phenomenon of concentration of these elements. In our research group, we have been studying the emanation of radon gas and its correlation to lead in soil in the region [29]. The presence of radon in the subsoil is an indication of alkaline igneous rocks and feldspathoids that present minerals with the content of uranium and that the lead in the aquifer is originated from radioisotopes generated in the series of radioactive decay of uranium.

The seasonality of copper in the aquifer was different and contrary to the results previously observed. The copper concentration increased exponentially in months that have the highest pluviometric level in the region and it decreases gradually during the months that follow the maximum peak in concentration. To analyze possible sources of copper in groundwater, reference materials about aquifer contamination correlated to economic activities and the land usage and occupation were consulted. Due to the observed characteristics, copper comes from a diffuse source originated by agricultural activity. The diffuse sources are characterized by presenting a wide area of contribution, deriving from activities that deposit pollutants sparsely, reaching bodies of water only in an intermittent way, associated with rainy periods [30,31]. The increment in copper concentration in groundwaters may have an origin in the leaching of agricultural chemicals through rainfall. The main economic base of the region is agribusiness, where it is most prominent the cultivation of sugar cane and yam. Agricultural inputs or subproducts employed with a corrective or nutritional purposed for both sugar cane and yam crops are copper salts-based [32]. Since we have no evidence of the contribution of the chemical elements of rain, further research should be done in the future to determine the composition of rain in the region and understand the contribution seasonal to underground water.

**Author Contributions:** Investigation, writing—original draft, L.A.M.; investigation, visualization, M.R.M.-S.; data curation, re-writing, statistical analysis, J.J.T.; conceptualization, methodology, validation, writing—review and editing, supervision, project administration, funding acquisition, M.F.S.T. All authors have read and agreed to the published version of the manuscript.

**Funding:** The authors acknowledge CEPID-FAPESP (2013/07296-2) and CNPq (301298/2017-3) for their financial support.

**Institutional Review Board Statement:** Not applicable.

**Informed Consent Statement:** Not applicable.

**Data Availability Statement:** The data that support the findings of this study are available from the corresponding author: MFST, upon request.

**Acknowledgments:** The authors would like to acknowledge SJT.

**Conflicts of Interest:** The authors declare no conflict of interest.

#### References

1. Cavazzana, G.H.; Lastoria, G.; Gabas, S.G. Surface-groundwater interaction in unconfined sedimentary aquifer system in the Brazil's tropical wet region. *RBRH-Rev. Bras. Recur.* **2019**, *24*. [[CrossRef](#)]
2. Machiwal, D.; Jha, M.K. Identifying sources of groundwater contamination in a hard-rock aquifer system using multivariate statistical analyses and GIS-based geostatistical modeling techniques. *J. Hydrol. Reg. Stud.* **2015**, *4*, 80–110. [[CrossRef](#)]
3. Guo, X.R.; Zuo, R.; Meng, L.; Wang, J.S.; Teng, Y.G.; Liu, X.; Chen, M.H. Seasonal and Spatial Variability of Anthropogenic and Natural Factors Influencing Groundwater Quality Based on Source Apportionment. *Int. J. Environ. Res. Public Health* **2018**, *15*, 279. [[CrossRef](#)] [[PubMed](#)]
4. Jayalakshmi, B.; Ramachandramoorthy, T.; Paulraj, A. Statistical interpretation on seasonal variations of groundwater quality in Ramanathapuram coastal tract, Tamil Nadu, India. *Environ. Earth Sci.* **2014**, *72*, 1271–1278. [[CrossRef](#)]

5. Dubrovsky, N.M.; Burow, K.R.; Gronberg, J.A.M. Effects of two contrasting agricultural land uses on shallow groundwater quality in the San Joaquin Valley, California: Design and preliminary interpretation. In *Models for Assessing and Monitoring Groundwater Quality*; IAHS Press: Wallingford, UK, 1995; pp. 49–58.
6. Frapporti, G.; Vriend, S.P.; Vangaans, P.F.M. Hydrogeochemistry of the Shallow Dutch Groundwater—Interpretation of the National Groundwater Quality Monitoring Network. *Water Resour. Res.* **1993**, *29*, 2993–3004. [[CrossRef](#)]
7. Adimalla, N.; Li, P.Y.; Venkatayogi, S. Hydrogeochemical Evaluation of Groundwater Quality for Drinking and Irrigation Purposes and Integrated Interpretation with Water Quality Index Studies. *Environ. Process.* **2018**, *5*, 363–383. [[CrossRef](#)]
8. Swamee, P.K.; Misra, A.K.; Poyil, R.P.; Choudhary, L.; Kaur, A.; Chintalapati, S. A linear and nonlinear approach for interpretation of groundwater quality based on water quality index. *Environ. Dev. Sustain.* **2018**, *20*, 2623–2642. [[CrossRef](#)]
9. Huntington, T.G. Evidence for intensification of the global water cycle: Review and synthesis. *J. Hydrol.* **2006**, *319*, 83–95. [[CrossRef](#)]
10. Oki, T.; Kanae, S. Global hydrological cycles and world water resources. *Science* **2006**, *313*, 1068–1072. [[CrossRef](#)]
11. Miyazawa, M.; Gimenez, S.M.N.; Yabe, M.J.S.; Oliveira, E.L.; Kamogawa, M.Y. Absorption and toxicity of copper and zinc in bean plants cultivated in soil treated with chicken manure. *Water Air Soil Pollut.* **2002**, *138*, 211–222. [[CrossRef](#)]
12. Jalali, M. Salinization of groundwater in arid and semi-arid zones: An example from Tajarak, western Iran. *Environ. Geol.* **2007**, *52*, 1133–1149. [[CrossRef](#)]
13. Subramani, T.; Rajmohan, N.; Elango, L. Groundwater geochemistry and identification of hydrogeochemical processes in a hard rock region, Southern India. *Environ. Monit. Assess.* **2010**, *162*, 123–137. [[CrossRef](#)]
14. Nriagu, J.O. A Silent Epidemic of Environmental Metal Poisoning. *Environ. Pollut.* **1988**, *50*, 139–161. [[CrossRef](#)]
15. Bodo, B.A. Heavy-Metals in Water and Suspended Particulates from an Urban Basin Impacting Lake-Ontario. *Sci. Total Environ.* **1989**, *87–88*, 329–344. [[CrossRef](#)]
16. Sakakibara, K.; Tsujimura, M.; Song, X.F.; Zhang, J. Spatiotemporal variation of the surface water effect on the groundwater recharge in a low-precipitation region: Application of the multi-tracer approach to the Taihang Mountains, North China. *J. Hydrol.* **2017**, *545*, 132–144. [[CrossRef](#)]
17. Rodriguez-Galiano, V.; Mendes, M.P.; Garcia-Soldado, M.J.; Chica-Olmo, M.; Ribeiro, L. Predictive modeling of groundwater nitrate pollution using Random Forest and multisource variables related to intrinsic and specific vulnerability: A case study in an agricultural setting (Southern Spain). *Sci. Total Environ.* **2014**, *476*, 189–206. [[CrossRef](#)]
18. Baez-Cazull, S.E.; McGuire, J.T.; Cozzarelli, I.M.; Voytek, M.A. Determination of dominant biogeochemical processes in a contaminated aquifer-wetland system using multivariate statistical analysis. *J. Environ. Qual.* **2008**, *37*, 30–46. [[CrossRef](#)]
19. Zheng, Y.; Chen, S.D.; Qin, H.P.; Jiao, J.J. Modeling the Spatial and Seasonal Variations of Groundwater Head in an Urbanized Area under Low Impact Development. *Water* **2018**, *10*, 803. [[CrossRef](#)]
20. Shamsudduha, M.; Chandler, R.E.; Taylor, R.G.; Ahmed, K.M. Recent trends in groundwater levels in a highly seasonal hydrological system: The Ganges-Brahmaputra-Meghna Delta. *Hydrol. Earth Syst. Sci.* **2009**, *13*, 2373–2385. [[CrossRef](#)]
21. Dubreuil, V.; Fante, K.P.; Planchon, O.; Neto, J.L.S. The types of annual climates in Brazil: An application of the classification of Koppen from 1961 to 2015. *Confins* **2018**, *37*. [[CrossRef](#)]
22. Stradioto, M.R.; Teramoto, E.H.; Chang, H.K. Rock-solute reaction mass balance of water flowing within an aquifer system with geochemical stratification. *Appl. Geochem.* **2020**, *123*, 104784. [[CrossRef](#)]
23. De Vries, J.J.; Simmers, I. Groundwater recharge: An overview of processes and challenges. *Hydrogeol. J.* **2002**, *10*, 5–17. [[CrossRef](#)]
24. McBride, G.B. *Using Statistical Methods for Water Quality Management: Issues, Problems and Solutions*; John Wiley & Sons Inc.: Chichester, UK, 2005; pp. 1–315. [[CrossRef](#)]
25. Wijngaard, R.R.; van der Perk, M.; van der Grift, B.; de Nijs, T.C.M.; Bierkens, M.F.P. The Impact of Climate Change on Metal Transport in a Lowland Catchment. *Water Air Soil Pollut.* **2017**, *228*, 107. [[CrossRef](#)]
26. Goncalves, V.F.M.; Manzione, R.L. Groundwater Recharge Estimates at Bauru Aquifer System (Bas). *Geo Uerj* **2019**. [[CrossRef](#)]
27. Liu, C.W.; Lin, K.H.; Kuo, Y.M. Application of factor analysis in the assessment of groundwater quality in a blackfoot disease area in Taiwan. *Sci. Total Environ.* **2003**, *313*, 77–89. [[CrossRef](#)]
28. Jiao, Y.F.; Liu, J.; Li, C.Z.; Qiu, Q.T.; Yu, X.Z.; Wang, W.; Zhang, G.J. Regulation storage calculation and capacity evaluation of the underground reservoir in the groundwater overdraft area of northern China. *Environ. Earth Sci.* **2020**, *79*, 18. [[CrossRef](#)]
29. Moreira-Silva, M.R.; Saenz, C.A.T.; Nunes, J.O.R.; Godoy, M.; Teixeira, M.F.S. Evidence for a correlation between total lead concentrations in soils and the presence of geological faults. *Environ. Chem. Lett.* **2017**, *15*, 481–488. [[CrossRef](#)]
30. Bendoricchio, G. Integrated management of water quality—The role of agricultural diffuse pollution sources. *Water Sci. Technol.* **1999**, *39*, vii.
31. Albek, E.A.; Goncu, S.; Uygun, B.S.; Albek, M.; Avdan, Z.Y.; Gungor, O. Water quality monitoring with emphasis on estimation of point and diffuse pollution sources. *Glob. Nest J.* **2019**, *21*, 163–171. [[CrossRef](#)]
32. Corbi, J.J.; Costa, C.G.; Gorni, G.R.; Colombo, V.; Rios, L. Environmental diagnosis of metals in streams near sugarcane cultivation areas: Current and historical analysis in the central region of the State of Sao Paulo. *An. Acad. Bras. Cienc.* **2018**, *90*, 2711–2719. [[CrossRef](#)] [[PubMed](#)]